ESC European Society of Cardiology

Cardiovascular Research (2024) **00**, 1–13
https://doi.org/10.1093/cvr/cvae070

Differential sex-dependent susceptibility to diastolic dysfunction and arrhythmia in cardiomyocytes from obese diabetic heart failure with preserved ejection fraction model

Juliana Mira Hernandez [1,2†], Erin Y. Shen[1†], Christopher Y. Ko [1], Zaynab Hourani[3], Emily R. Spencer [1], Daria Smoliarchuk[1], Julie Bossuyt [1], Henk Granzier [3], Donald M. Bers [1*], and Bence Hegyi [1*]

[1]Department of Pharmacology, University of California, 451 Health Sciences Drive, Davis, CA 95616, USA; [2]Research Group Biogenesis, Faculty of Agricultural Sciences, Veterinary Medicine, University of Antioquia, Medellin, Colombia; and [3]Department of Cellular and Molecular Medicine, University of Arizona, Tucson, AZ 85721, USA

Received 16 August 2023; revised 29 February 2024; accepted 17 March 2024; online publish-ahead-of-print 26 April 2024

Time of primary review: 21 days

Aims

Sex differences in heart failure with preserved ejection fraction (HFpEF) are important, but key mechanisms involved are incompletely understood. While animal models can inform about sex-dependent cellular and molecular changes, many previous pre-clinical HFpEF models have failed to recapitulate sex-dependent characteristics of human HFpEF. We tested for sex differences in HFpEF using a two-hit mouse model (leptin receptor–deficient *db/db* mice plus aldosterone infusion for 4 weeks; *db/db* + Aldo).

Methods and results

We performed echocardiography, electrophysiology, intracellular Ca^{2+} imaging, and protein analysis. Female HFpEF mice exhibited more severe diastolic dysfunction in line with increased titin N2B isoform expression and PEVK element phosphorylation and reduced troponin-I phosphorylation. Female HFpEF mice had lower BNP levels than males despite similar comorbidity burden (obesity, diabetes) and cardiac hypertrophy in both sexes. Male HFpEF mice were more susceptible to cardiac alternans. Male HFpEF cardiomyocytes (vs. female) exhibited higher diastolic [Ca^{2+}], slower Ca^{2+} transient decay, reduced L-type Ca^{2+} current, more pronounced enhancement of the late Na^{+} current, and increased short-term variability of action potential duration (APD). However, male and female HFpEF myocytes showed similar downregulation of inward rectifier and transient outward K^{+} currents, APD prolongation, and frequency of delayed afterdepolarizations. Inhibition of Ca^{2+}/calmodulin-dependent protein kinase II (CaMKII) reversed all pathological APD changes in HFpEF in both sexes, and empagliflozin pre-treatment mimicked these effects of CaMKII inhibition. Vericiguat had only slight benefits, and these effects were larger in HFpEF females.

Conclusion

We conclude that the *db/db* + Aldo pre-clinical HFpEF murine model recapitulates key sex-specific mechanisms in HFpEF and provides mechanistic insights into impaired excitation–contraction coupling and sex-dependent differential arrhythmia susceptibility in HFpEF with potential therapeutic implications. In male HFpEF myocytes, altered Ca^{2+} handling and electrophysiology aligned with diastolic dysfunction and arrhythmias, while worse diastolic dysfunction in females may depend more on altered myofilament properties.

* Corresponding authors. Tel: +1 530 752 9962; fax: +1 530 752 7710, E-mail: bhegyi@ucdavis.edu (B.H.); Tel: +1 530 752 6517; fax: +1 530 752 7710, Email: dmbers@ucdavis.edu (D.M.B.)
† The first two authors contributed equally to the study.

Graphical Abstract

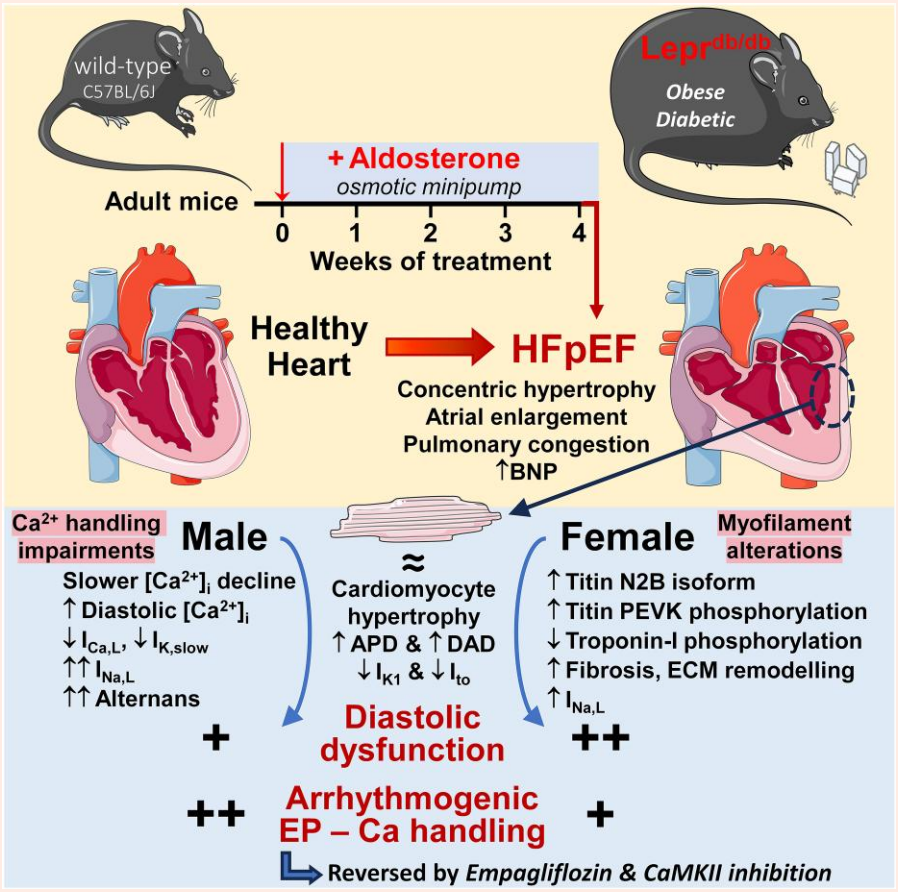

Keywords HFpEF • Sex differences • Arrhythmia • Diastolic dysfunction • CaMKII

1. Introduction

Sex differences in cardiovascular diseases are increasingly recognized, yet females are underrepresented in clinical trials, and mechanisms remain incompletely understood.[1–4] Pre-menopausal women have lower risk of coronary artery disease (CAD) and reduced susceptibility to ischaemic heart injury.[1] The female heart is also relatively protected against heart failure (HF) with reduced ejection fraction (HFrEF), and this protection wanes post-menopause.[2,3] In contrast to CAD and HFrEF, heart failure with preserved ejection fraction (HFpEF) is more prevalent in both pre-menopausal and post-menopausal women.[2,5,6] This might be due to the common extracardiac comorbidities that markedly increase the risk of developing HFpEF in women.[7] Hypertension increases HF risk by three-fold in women compared with two-fold in men,[8] and diabetes mellitus increases HF risk by five-fold in women compared with 2.4-fold in men.[9] The disease prognosis and diastolic dysfunction in HFpEF have also been reported worse in females.[6] In contrast to higher susceptibility of female patients for contractile dysfunction, cardiac arrhythmia and sudden cardiac death (SCD) might be more frequent in male patients with HFpEF.[10] SCD incidence was 2.1-fold higher in male vs. female patients with HFpEF in the Treatment of Preserved Cardiac Function Heart Failure with an Aldosterone Antagonist (TOPCAT) trial.[11] However, exact arrhythmia risk and mechanisms in HFpEF remain unclear.[12]

Animal models can provide important mechanistic insights into sex-dependent disease mechanisms[13]; however, female animals are underutilized in pre-clinical cardiovascular research.[14] Several mouse models that exhibit aspects of HFpEF have been previously used; however, many models fall short of recapitulating the complex, multiorgan HFpEF phenotype seen in human patients.[15,16] Recently, two-(or multi)-hit models have emerged, combining metabolic and haemodynamic stresses, and showed multiple characteristics of human HFpEF.[17] Among these models, a mouse model using high-fat diet (HFD) and N^{ω}-nitro-L-arginine methyl ester (L-NAME), an inhibitor of nitric oxide (NO) synthases, quickly became popular allowing translational investigations in HFpEF.[18–20] However, female sex is protective against developing HFpEF in the HFD + L-NAME–treated mice,[21] which contrasts with clinical observations in human HFpEF. Because HFpEF represents a diverse group of patients, multiple models with different underlying pathophysiology may be required to better understand HFpEF.[12,22] Recently, we established another two-hit model of HFpEF that synergistically combines the leptin receptor–deficient *db/db* mice with 4-week continuous aldosterone (Aldo) infusion (*db/db* + Aldo), which mimics a more diabetic sub-phenogroup in HFpEF.[23] Importantly, diastolic dysfunction is more prominent in female patients with diabetes and HFpEF[24] and in female *db/db* mice,[25] and mineralocorticoid receptor inhibition may provide more benefit in female patients with HFpEF.[26] Thus, we hypothesized that the *db/db* + Aldo mice may better recapitulate sex differences in human HFpEF, with worse diastolic dysfunction in females. Additionally, we aimed to characterize sex-dependent changes in intracellular Ca^{2+} handling and electrophysiology in HFpEF cardiomyocytes, because sex-specific proarrhythmia mechanisms in HFpEF are largely unknown. We also focused on select myofilament proteins, titin and troponin-I. We then tested for sex-specific cardiomyocyte

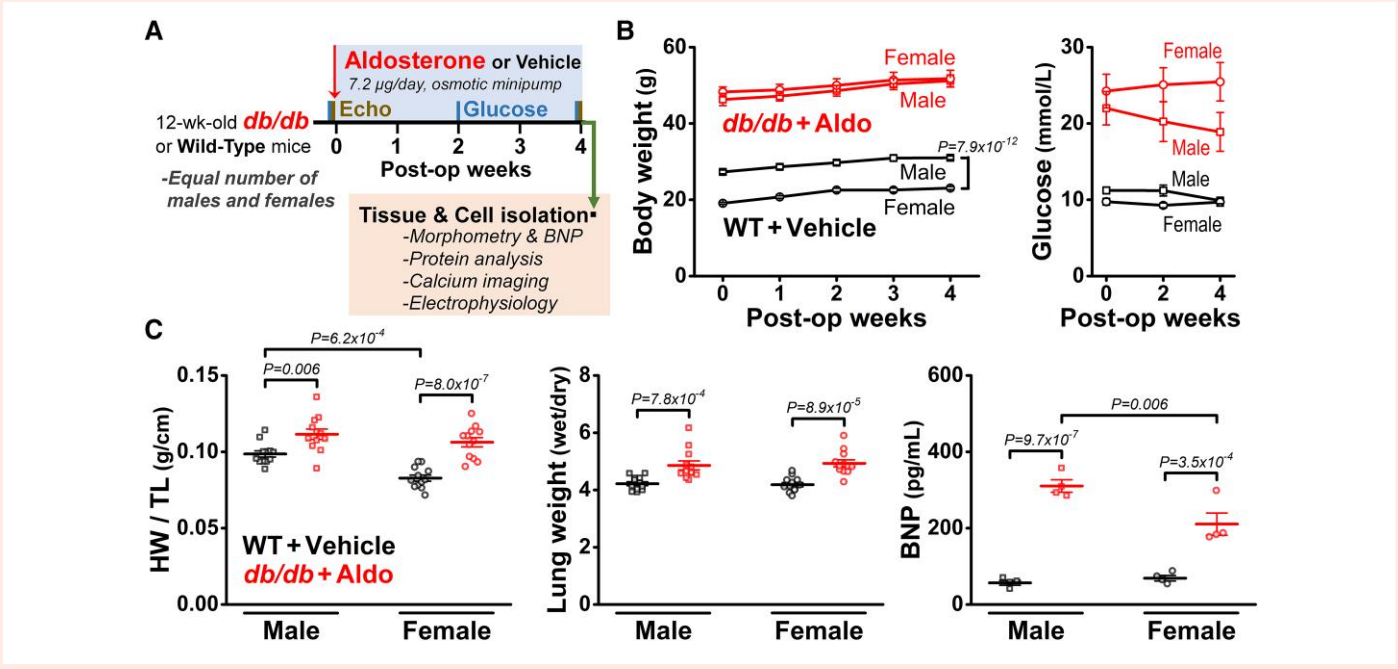

Figure 1 Sex differences in morphometric parameters in HFpEF mice. (*A*) HFpEF study protocol and assessment of extracardiac morbidities, heart function, and cardiomyocyte excitation–contraction coupling and electrophysiology. (*B*) Sex-dependent changes in body weight and blood glucose levels over time in *db/db* mice with chronic aldosterone infusion (*db/db* + Aldo) vs. vehicle-treated WT control (WT + vehicle). Two-way repeated measures ANOVA with Geisser–Greenhouse correction. (*C*) Sex-dependent cardiac hypertrophy, pulmonary oedema, and increased BNP plasma levels in *db/db* + Aldo vs. WT + vehicle (HW/TL, heart weight to tibial length ratio; BNP, B-type natriuretic peptide). Two-way ANOVA followed by Šídák's multiple comparisons test. $N = 12$ animals/experimental group except for BNP measurements where $N = 4$.

electrophysiological responses to sodium–glucose cotransporter-2 (SGLT2) inhibitor empagliflozin (an established drug in HFpEF),[27] soluble guanylate cyclase (sGC) stimulator vericiguat (a drug with ample preclinical data but that failed in HFpEF clinical trials),[28] and inhibition of Ca^{2+}/calmodulin-dependent kinase II (CaMKII, a key signalling molecule regulating cardiomyocyte excitation–contraction coupling and multiple ion channels)[29] using autocamtide-2-related inhibitory peptide (AIP) to advance clinical translation.

2. Methods

All animal handling and laboratory procedures were in accordance with the approved protocols of the Institutional Animal Care and Use Committee at University of California, Davis (#23175), conforming to the Guide for the Care and Use of Laboratory Animals published by the US National Institutes of Health (8th edition, 2011). An expanded Methods section is available in the Supplementary material.

2.1 Animal procedures

Adult (10-week-old) $Lepr^{db/db}$ (strain #000697) and corresponding wild-type (WT) mice on C57BL/6J background were obtained from The Jackson Laboratory. Mice were kept at standard temperature, humidity, and lighting. Food (Teklad, 2018) and drinking water were provided *ad libitum*. Osmotic minipumps (Alzet, 2004) were implanted subcutaneously in 12-week-old mice that delivered a continuous infusion of either D-aldosterone (0.3 µg/h) or vehicle (saline with 5% ethanol) for 4 weeks (study protocol is shown in *Figure 1A*). We used block randomization with a block size of four animals (for each genotype, treatment, and sex), with 24 control (WT + vehicle) and 24 two-hit (*db/db* + Aldo) mice included (allowing for detailed isolated myocyte studies), and for the one-hit controls, we used 8 WT + Aldo and 8 *db/db* + vehicle mice. For proper allocation concealment, animals were recruited blinded based on sequential ear tag numbers randomly assigned by the animal housing staff. Each treatment group included equal numbers of male and female animals. Animals were injected with heparin (400 U/kg) and were subjected to general anaesthesia by 2–5% isoflurane inhalation in 100% oxygen throughout the terminal surgical procedure. All animals were euthanized by surgical excision of the heart while in deep anaesthesia. Enzymatic isolation of cardiomyocytes was performed as previously described.[30]

2.2 Blood glucose and BNP measurements

Blood glucose levels were measured in blood samples collected from the middle tail vein using OneTouch UltraMini blood glucose monitoring system and test strips (LifeScan). B-type natriuretic peptide (BNP) levels were measured in blood plasma by ELISA (RayBiotech, EIAM-BNP-1).

2.3 Echocardiography

Transthoracic echocardiography was performed in anaesthetized (isoflurane, 0.5–3%) animals. M-mode and Doppler images were acquired using a Vevo 2100 echocardiography system (FUJIFILM VisualSonics) equipped with a 40 MHz transducer.

2.4 Protein analysis

Gel electrophoresis and immunoblotting were performed to determine changes in titin isoform expression and phosphorylation, troponin-I phosphorylation (pTnI), and periostin expression.

2.5 Myocyte Ca^{2+} imaging and electrophysiology

Intracellular Ca^{2+} signals were measured using confocal microscopy in freshly isolated ventricular cardiomyocytes loaded with Fluo-4 AM at

21–22°C. Action potentials (APs) and ionic currents were recorded in isolated ventricular cardiomyocytes via patch-clamp technique at 37°C.

2.6 Statistics

Data are presented as mean ± SEM. Normality of the data and the equality of group variance were assessed by Shapiro–Wilk and Brown–Forsythe tests, respectively. Statistical significance of differences was determined using two-way ANOVA followed by appropriate *post hoc* tests in pairwise comparisons. Hierarchical statistical analyses (nested tests) to account for intersubject variability and non-independent sampling (as multiple cells may come from one animal) were performed in cellular experiments. GraphPad Prism 10 was used for data analysis. A $P < 0.05$ was considered statistically significant.

3. Results

3.1 Sex differences in multiorgan function for HFpEF induced by diabetes and excess aldosterone

First, we compared morphometric and metabolic parameters (*Figure 1*) between male and female mice in the *db/db* + Aldo two-hit model of HFpEF vs. vehicle-treated WT controls (WT + vehicle) and in the one-hit disease models (*db/db* or aldosterone infusion alone; Supplementary material online, *Figure S1*). All *db/db* + Aldo mice showed marked obesity, hyperglycaemia, cardiac hypertrophy, pulmonary congestion, and elevated plasma BNP levels (*Figure 1B* and *C*), all similar to our prior work on this HFpEF model.[23] Body weights of female *db/db* + Aldo mice were similar to the obese males, and the female *db/db* + Aldo mice had a tendency for higher blood glucose levels, especially later during aldosterone infusion (*Figure 1B*). Cardiac hypertrophy and pulmonary oedema were not different in female and male *db/db* + Aldo mice. Note that the heart and body weights were smaller in control female mice than in males, making the HFpEF-induced relative increases larger in females. Importantly, female *db/db* + Aldo mice had significantly lower plasma BNP levels (*Figure 1C*), indicating a diminished BNP upregulation in HFpEF females ($P = 0.007$ for interaction between sex and HFpEF in two-way ANOVA test). In vehicle-treated *db/db* mice (*db/db* + vehicle) or aldosterone-treated WT mice (WT + Aldo), no significant increase in cardiac hypertrophy, pulmonary oedema, or BNP levels were found, and no sex difference therein was observed (see Supplementary material online, *Figure S1*) indicating that HFpEF develops via the synergistic action between *db/db* and aldosterone treatment.

3.2 Marked diastolic dysfunction, especially in female HFpEF

Echocardiographic evaluation showed preserved ejection fraction (EF) in all treatment groups (*Figure 2*, Supplementary material online, *Figure S2*). Concentric cardiac hypertrophy was evident from left ventricular (LV) wall thickening and increase in LV remodelling index (LVRI, a ratio between LV mass and LV internal diameter) in both male and female *db/db* + Aldo mice (*Figure 2B*). However, the diastolic dysfunction (*Figure 2C*), characterized by marked increases in E/A and E/e′ echo Doppler indexes, was more pronounced in female *db/db* + Aldo mice than in males (E/e′, $P = 3.8 \times 10^{-6}$ for interaction between sex and HFpEF). Left atrial enlargement (*Figure 2C*) was also more pronounced in female *db/db* + Aldo mice ($P = 0.008$ for interaction between sex and HFpEF). In the one-hit versions of this heart disease model (*db/db* + vehicle and WT + Aldo), no significant sex difference in any echocardiographic parameters was found (see Supplementary material online, *Figure S2*). These functional characteristics demonstrate that the female sex is associated with worse diastolic dysfunction in the *db/db* + Aldo HFpEF mouse model, similar to human HFpEF.

3.3 Diastolic Ca^{2+} handling impairment, especially in male HFpEF

Impaired Ca^{2+} handling contributes to contractile dysfunction and arrhythmias in HFrEF[31]; however, little is known about Ca^{2+} handling impairments in HFpEF. Thus, we performed Ca^{2+} imaging in isolated ventricular myocytes loaded with the fluorescent intracellular Ca^{2+} indicator, Fluo-4 AM (*Figure 3A*). The amplitude of the intracellular [Ca^{2+}] transient (CaT) at 1 Hz pacing was unchanged in both male and female *db/db* + Aldo cardiomyocytes (*Figure 3B*) consistent with the preserved systolic function on echocardiography (*Figure 2B*). However, the diastolic [Ca^{2+}] in paced cells, quantified as the ratio of minimum F between consecutive beats and the resting F_0, was increased only in male but not female *db/db* + Aldo, in line with prolonged CaT decay τ in male *db/db* + Aldo (*Figure 3C*). At 2 Hz pacing, HFpEF myocytes showed similar frequency-dependent acceleration of CaT decay as healthy controls; however, male *db/db* + Aldo myocytes still showed prolonged CaT decay τ with a more pronounced increase in diastolic [Ca^{2+}] (see Supplementary material online, *Figure S3A*). The sarcoplasmic reticulum (SR) Ca^{2+} load (*Figure 3C*) and the Ca^{2+} spark rate (see Supplementary material online, *Figure S3B*) were unchanged in both male and female *db/db* + Aldo myocytes. These data indicate that impaired Ca^{2+} handling (slower SR Ca^{2+} reuptake but unchanged SR Ca^{2+} leak) may contribute to diastolic dysfunction, but particularly in HFpEF males.

3.4 Myofilament alterations are enhanced in female HFpEF

Molecular determinants of diastolic dysfunction have been further tested for select myofilament alterations in HFpEF. Isoform expression analysis of the giant elastic protein titin revealed a slight increase of the shorter and stiffer N2B isoform relative to total titin in female but not in male *db/db* + Aldo ventricles (*Figure 4A*). Post-translational modifications, including phosphorylation of titin in the PEVK (named after its enrichment in proline, glutamic acid, valine, and lysine) spring element, can affect myocyte stiffness.[32] Phosphorylation of the key PEVK serine 170 site (pS170, corresponding to S12022 in full-length human titin, target for protein kinase C and CaMKII)[32,33] was significantly increased in female but not in male *db/db* + Aldo ventricles (*Figure 4B*). pTnI at serine 22/23 was significantly increased in *db/db* + Aldo males, indicating desensitization of myofilament Ca^{2+} responsiveness. However, there was a trend for reduced TnI phosphorylation in *db/db* + Aldo females, which could increase myofilament Ca^{2+} sensitivity (*Figure 4C*), resulting in elevated force as $[Ca^{2+}]_i$ declines during diastole. Periostin, an activated fibroblast marker and key regulator,[34] showed a trend towards higher expression in female *db/db* + Aldo ventricles (see Supplementary material online, *Figure S4*). These data indicate that changes in contractile filaments and tissue structure may be the dominant mechanisms for the greater relaxation deficit in HFpEF females.

3.5 Arrhythmogenic APs in male HFpEF

Contractile dysfunction and Ca^{2+} handling impairments are associated with alterations in cardiac APs that increase the risk of cardiac arrhythmias.[35] Thus, we measured APs in isolated ventricular myocytes (*Figure 5A*). The AP durations at 20, 50, 75, and 90% repolarization (APD_{20}, APD_{50}, APD_{75}, and APD_{90}) were calculated to analyse repolarization dynamics. The early AP repolarization (APD_{20} and APD_{50}) was slightly prolonged only in male *db/db* + Aldo; however, APD_{75} and APD_{90} were both markedly prolonged in *db/db* + Aldo myocytes, similarly both in males and females (*Figure 5B*, Supplementary material online, *Figure S5*). The resting membrane potential and maximal upstroke velocity showed trends for a slight reduction in *db/db* + Aldo (see Supplementary material online, *Figure S5*). The short-term variability (STV) of APD_{90} was significantly increased in *db/db* + Aldo (*Figure 5C*) with a larger increase in males ($P = 0.025$ for interaction between sex and HFpEF; *Figure 5D*). Moreover, *db/db* + Aldo myocytes also showed APD_{90} alternans at rapid pacing frequencies (*Figure 5E*). Interestingly, male *db/db* + Aldo myocytes exhibited larger amplitude of APD_{90} alternans at matching APD_{90} (and diastolic intervals) than females

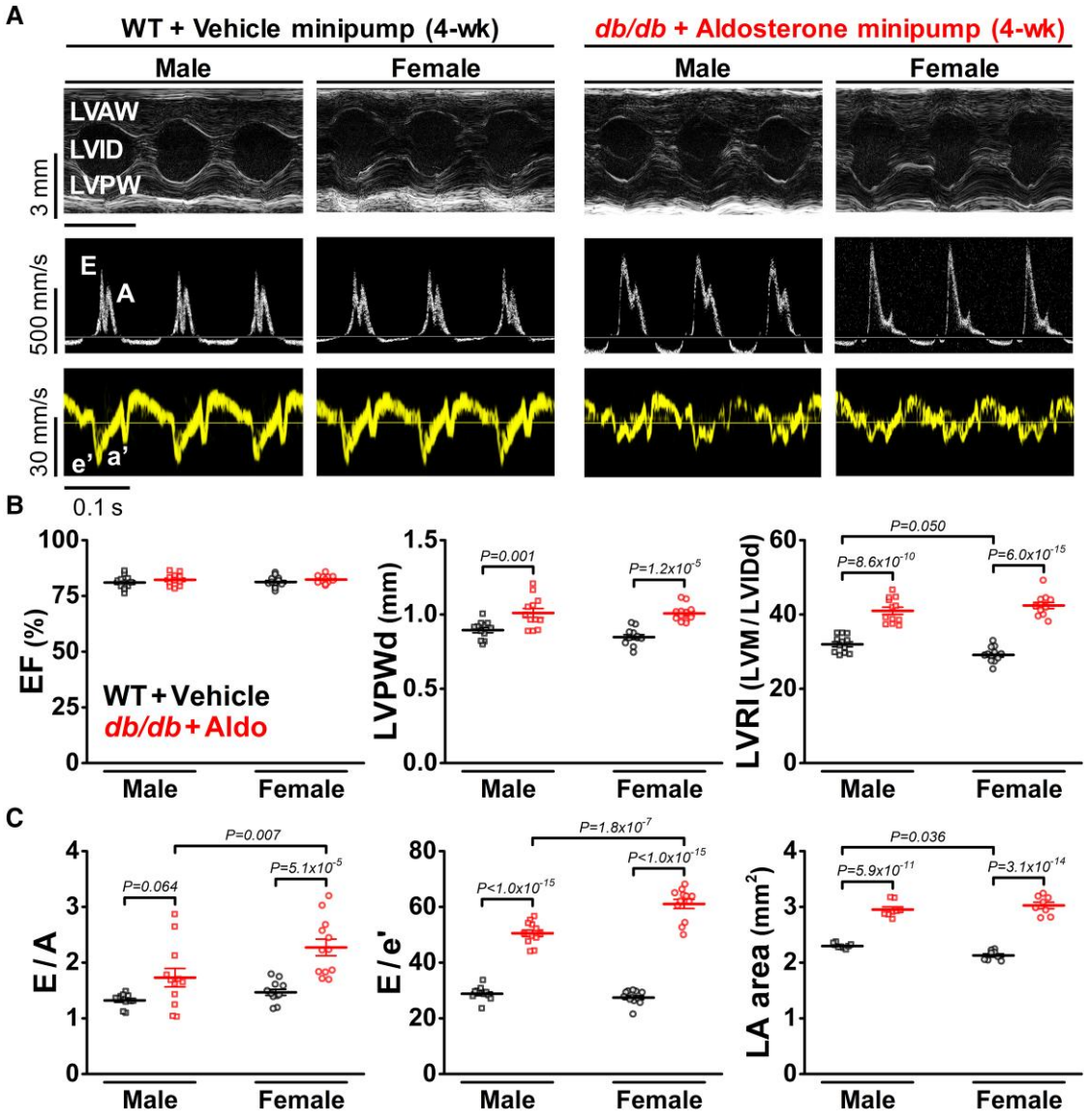

Figure 2 More severe diastolic dysfunction in female HFpEF mice. (*A*) LV M-mode, flow, and tissue Doppler echocardiographic images in male and female *db/db* mice with chronic aldosterone infusion (*db/db* + Aldo) vs. vehicle-treated WT control (WT + vehicle), 4 weeks after minipump implantation. (*B*) Preserved EF, cardiac hypertrophy, and increased LVRI (a ratio between LV mass and LV internal diameter) in both sexes in *db/db* + Aldo mice (LVPWd, LV end-diastolic posterior wall thickness; LVM, LV mass; LVIDd, LV internal diameter in diastole). (*C*) More severe LV diastolic dysfunction and left atrial (LA) area enlargement in female *db/db* + Aldo mice. (E/A, ratio between mitral E-wave and A-wave; E/e′, ratio between mitral E-wave and e′-wave). Two-way ANOVA followed by Šídák's multiple comparisons test. $N = 12$ animals in each group except for LA area where $N = 8$.

(*Figure 5E* and *F*), consistent with a dominant Ca^{2+}-driven mechanism for alternans formation.[36]

In line with the increased susceptibility for APD_{90} alternans, we also observed contractile alternans in echocardiograms in awakening *db/db* + Aldo animals *in vivo* (at heart rates of ≈600 b.p.m.) but not in any control animals (see Supplementary material online, *Figure S6*). The magnitude of alternating changes in LV systolic and diastolic diameters in subsequent beats was significantly larger in male than in female *db/db* + Aldo animals (see Supplementary material online, *Figure S6*). In ventricular myocytes, delayed afterdepolarizations (DADs) were also enhanced in *db/db* + Aldo following cessation of tachypacing; however, this increase was similar in males and females (see Supplementary material online, *Figure S7*). These data are in line with the increased arrhythmia risk in HFpEF males. The dominant sex-dependent differences in cellular arrhythmia mechanisms in HFpEF were the increase in alternans susceptibility and larger STV in males, both favouring re-entry mechanisms in the heart.

3.6 Sex differences in ionic current remodelling in HFpEF

We then performed voltage-clamp experiments to measure ionic currents that mediate APD alterations in HFpEF. The membrane capacitance was significantly increased in both male and female HFpEF myocytes (*Figure 6A*), indicating similar cardiomyocyte hypertrophy in both sexes and paralleling the observed overall cardiac hypertrophy (*Figure 1C*). Because the AP repolarization was impaired and remodelling in K^+

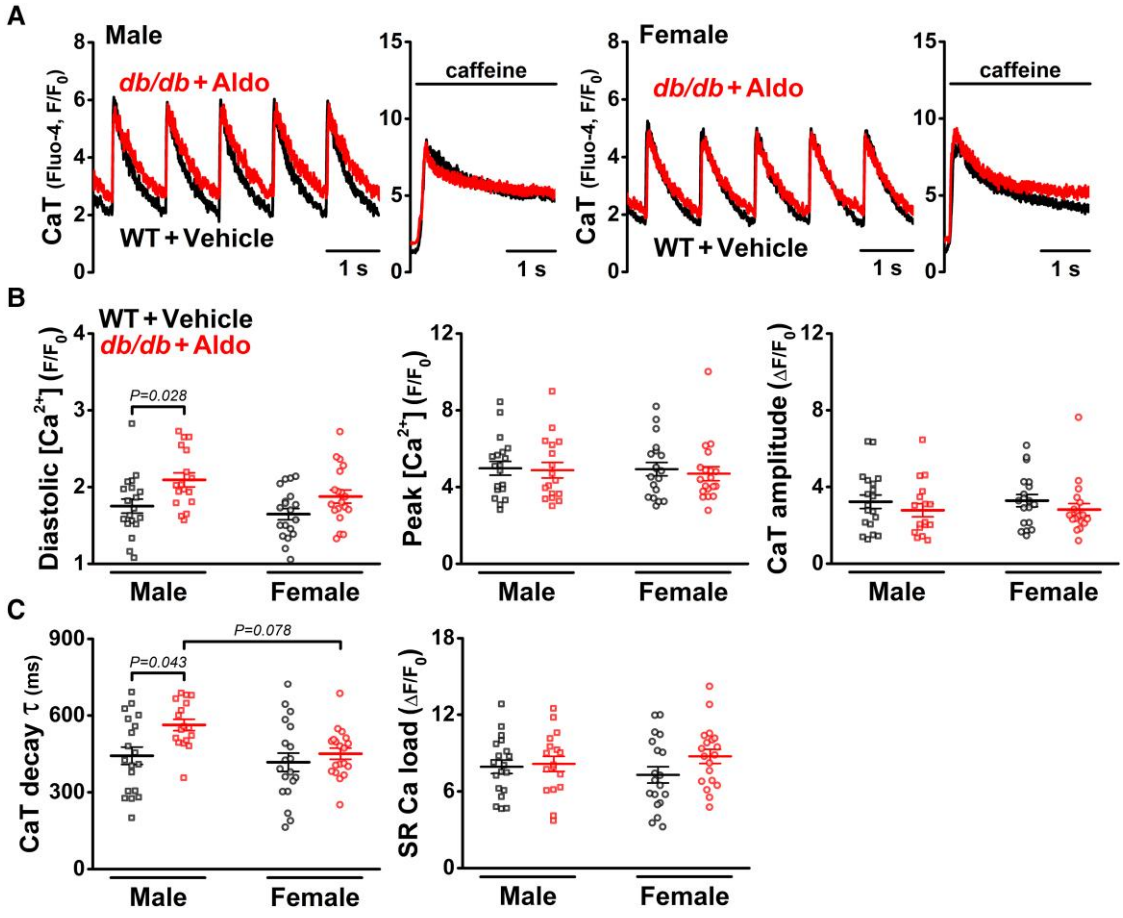

Figure 3 Sex differences in intracellular Ca^{2+} handling in HFpEF cardiomyocytes. (*A*) Intracellular Ca^{2+} signals in *db/db* mice with chronic aldosterone infusion (*db/db* + Aldo) vs. vehicle-treated WT control (WT + vehicle) cardiomyocytes paced at 1 Hz and during rapid caffeine application. (*B*) Intracellular Ca^{2+} transient (CaT) parameters. Diastolic [Ca^{2+}] is the ratio of minimum F between beats at 1 Hz pacing and the resting F_0. (*C*) CaT decay tau and SR Ca^{2+} content (assessed by rapid local application of 10 mmol/L caffeine). *n* (cells)/*N* (animals) = 19/8 for WT + vehicle male, 19/7 for WT + vehicle female, 17/8 for *db/db* + Aldo male, and 19/7 for *db/db* + Aldo female. Hierarchical (nested) ANOVA followed by Šídák's multiple comparisons test.

channels has been implicated in HFpEF,[37] we first measured repolarizing K^+ currents. The inward rectifier K^+ current (I_{K1}) density (*Figure 6A*) was significantly reduced in *db/db* + Aldo, similarly in males and females, with reductions at both −140 mV (inward I_{K1}) and −40 mV (outward I_{K1}), which would enhance DAD amplitude. The net voltage-gated K^+ current (I_{Kv}) was also markedly downregulated in both male and female *db/db* + Aldo myocytes (*Figure 6B*). To gain further insights, I_{Kv} components were separated by biexponential fitting to the current decay under a long (4.5 s) depolarizing voltage pulse (*Figure 6C*). The transient outward K^+ current (I_{to}) was downregulated in *db/db* + Aldo myocyte in both sexes. The slowly inactivating K^+ current ($I_{K,slow}$) was significantly reduced only in male *db/db* + Aldo myocytes. The sustained K^+ current (I_{SUS}) measured at the end of the voltage pulse did not change in *db/db* + Aldo myocytes.

We then measured the major depolarizing currents during the AP, the L-type Ca^{2+} current ($I_{Ca,L}$) and late Na^+ current ($I_{Na,L}$). Interestingly, $I_{Ca,L}$ was downregulated in male *db/db* + Aldo myocytes and unchanged in females (*Figure 6D*). In contrast to $I_{Ca,L}$, $I_{Na,L}$ was markedly upregulated in *db/db* + Aldo (*Figure 6E*). This $I_{Na,L}$ upregulation, however, was more pronounced in male *db/db* + Aldo ($P = 0.026$ for interaction between sex and HFpEF). These data show differential sex-specific remodelling in ionic currents in HFpEF, which underlies APD changes and contributes to sex-dependent arrhythmia susceptibility more collectively in HFpEF males.

3.7 Empagliflozin and CaMKII inhibition suppress arrhythmic APD changes in HFpEF

Sex differences in therapeutic responses are incompletely understood and may be important in HFpEF.[5,26] Cell pre-treatment with the SGLT2 inhibitor empagliflozin fully reversed all arrhythmogenic APD changes (i.e. APD_{90} prolongation, increased STV, APD alternans, and DADs) both in male and female *db/db* + Aldo myocytes (*Figure 7*, Supplementary material online, *Figure S8*). AIP, a selective CaMKII inhibitor, mimicked these effects and was similarly effective in reversing APD changes in both HFpEF males and females (*Figure 7*). Vericiguat, a stimulator of sGC that enhances protein kinase G (PKG) signalling, significantly attenuated APD_{90} prolongation, reduced STV, and reduced DAD frequency in female *db/db* + Aldo myocytes (*Figure 7*, Supplementary material online, *Figure S8*). However, the effect size of vericiguat was smaller than that of empagliflozin and AIP in female *db/db* + Aldo myocytes (*Figure 7*). In contrast to females, in male *db/db* + Aldo myocytes, vericiguat failed to alter STV, APD alternans, and DADs and only slightly attenuated APD_{90} prolongation (*Figure 7*, Supplementary material online, *Figure S8*). Notably, none of these drugs influenced APD_{90}, STV, APD alternans, or DAD frequency in vehicle-treated WT controls (see Supplementary material online, *Figure S9*). These data show that empagliflozin and AIP had marked effects on cardiomyocyte electrophysiology in HFpEF, and they provided similar benefits both in

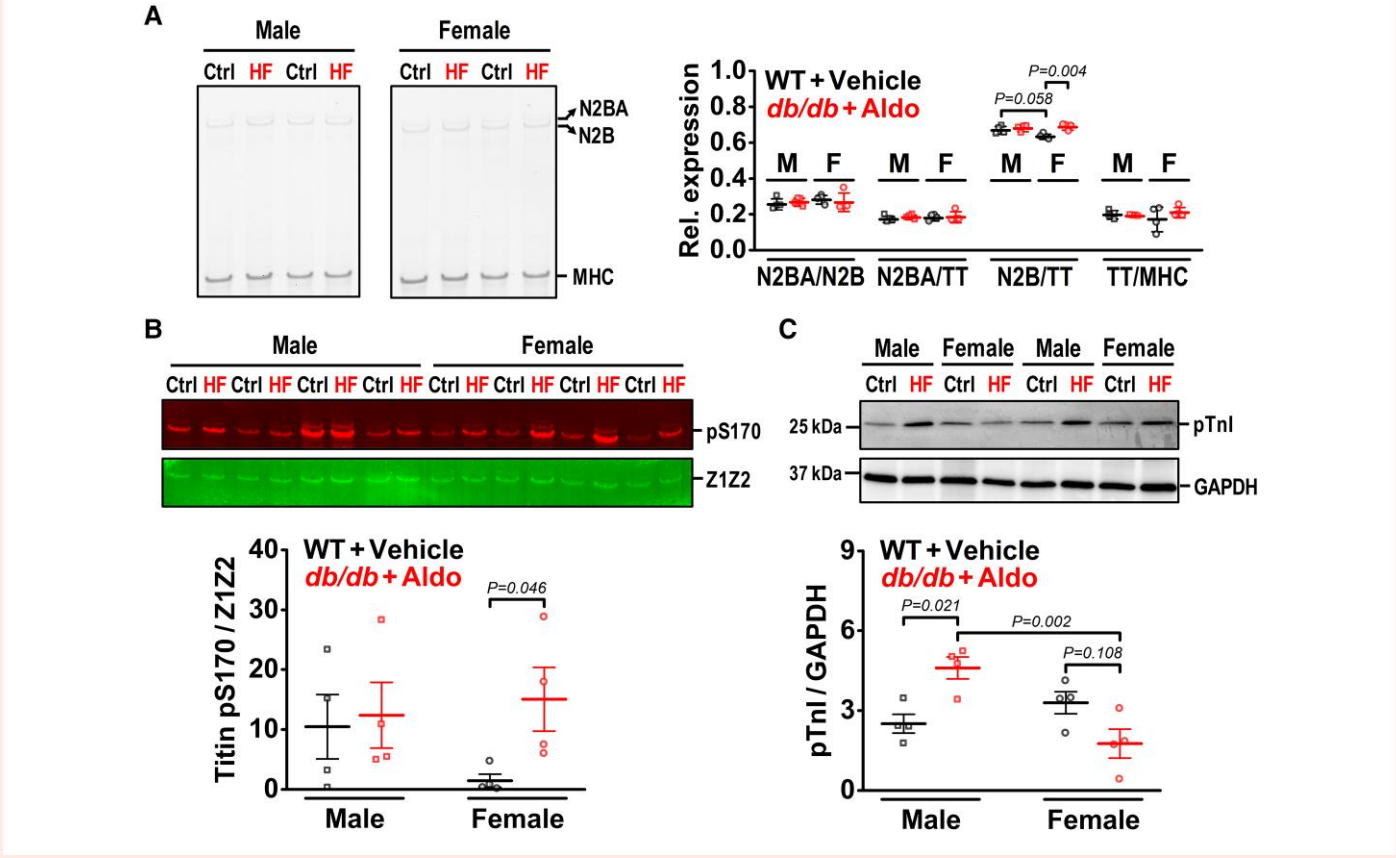

Figure 4 Sex differences in myofilament alterations in HFpEF ventricles. (*A*) Titin isoform analysis in male (M) and female (F) *db/db* + Aldo HFpEF (HF) vs. vehicle-treated WT control (Ctrl) ventricular samples. Relative expression of the more compliant N2BA and the stiffer N2B titin isoform to total titin (TT) and myosin heavy chain (MHC) was assessed using gel electrophoresis. ANOVA followed by Šídák's multiple comparisons test. (*B*) Western blot data showing increased phosphorylation of serine 170 of titin's PEVK domain normalized to titin Z1Z2 element (to assess total intact titin level) in *db/db* + Aldo females. Kruskal–Wallis ANOVA followed by Dunn's multiple comparisons test. (*C*) pTnI normalized to glyceraldehyde 3-phosphate dehydrogenase (GAPDH). ANOVA followed by Šídák's multiple comparisons test. Three technical replicates (blots) were performed for each protein sample. $N = 4$ animals in each group.

males and females, whereas vericiguat provided minor benefits on cardiomyocyte electrophysiology only in females.

4. Discussion

Here, we report that the *db/db* + Aldo HFpEF murine model recapitulates key sex differences seen in human HFpEF, including more severe diastolic dysfunction (*Figure 2*) and myofilament alterations (*Figure 4*) in females and higher arrhythmia susceptibility in males in the form of cardiac alternans (*Figure 5*, Supplementary material online, *Figure S6*), a beat-to-beat periodic alternation in electrical activity, and contractile strength that is associated with high risk of ventricular fibrillation and SCD.[36] These sex differences occurred under similar comorbidity burden (obesity, diabetes), cardiac hypertrophy, atrial enlargement, and pulmonary congestion in HFpEF males and females (*Figures 1* and *2*). HFpEF cardiomyocytes showed marked APD prolongation, enhanced DADs, and increased STV and alternans at physiological pacing rates (*Figure 5*). APD alternans and STV had larger magnitudes in HFpEF males vs. females, despite similar APD prolongation (which by itself can increase alternans susceptibility and STV) in both sexes. This suggests impaired excitation-contraction coupling and Ca^{2+}-dependent feedback signals that could further augment APD alternans and STV.[36,38,39] Indeed, male HFpEF cardiomyocytes exhibited higher diastolic [Ca^{2+}], slower CaT decay, reduced $I_{Ca,L}$, and larger $I_{Na,L}$ enhancement (*Figures 3* and *6*). However, downregulation of I_{K1} and I_{to} were similar in HFpEF males and females (*Figure 6*). Myocyte pre-treatment with the specific CaMKII inhibitor, AIP, fully reversed all arrhythmogenic APD changes in both sexes in HFpEF, indicating a pivotal role for CaMKII in HFpEF proarrhythmia (*Figure 7*). Importantly, these effects were mimicked by empagliflozin in both sexes in HFpEF, suggesting that empagliflozin could attenuate pathological CaMKII signalling (*Figure 7*). Vericiguat had only slight benefits, and these effects were larger in HFpEF females, in line with lower BNP levels that could attenuate sGC activation and PKG signalling in HFpEF females (*Figure 7*).

Since obesity and diabetes are among the frequent comorbidities in HFpEF, and mineralocorticoid receptor antagonism showed benefits, especially in obese female patients with HFpEF,[26] we first proposed the *db/db* + Aldo model, in which the *db/db* phenotype–mediated metabolic stress is combined with chronic aldosterone excess to synergistically promote HFpEF.[23] In fact, diabetes and high aldosterone levels are associated with worse outcomes in patients with HFpEF.[40] Aldosterone levels are increased in parallel with abnormalities of LV structure and geometry in patients with HFpEF, particularly in females.[41] The leptin receptor–deficient C57BL/6J *db/db* mice exhibit not only severe hyperinsulinaemia and type 2 diabetes but also hyperleptinaemia.[42] The leptin–aldosterone–neprilysin axis has been implicated in HFpEF, and female sex is associated with higher levels of aldosterone, leptin, and neprilysin and a decrease in the counterbalancing effects of natriuretic peptides.[43] In line with these observations in

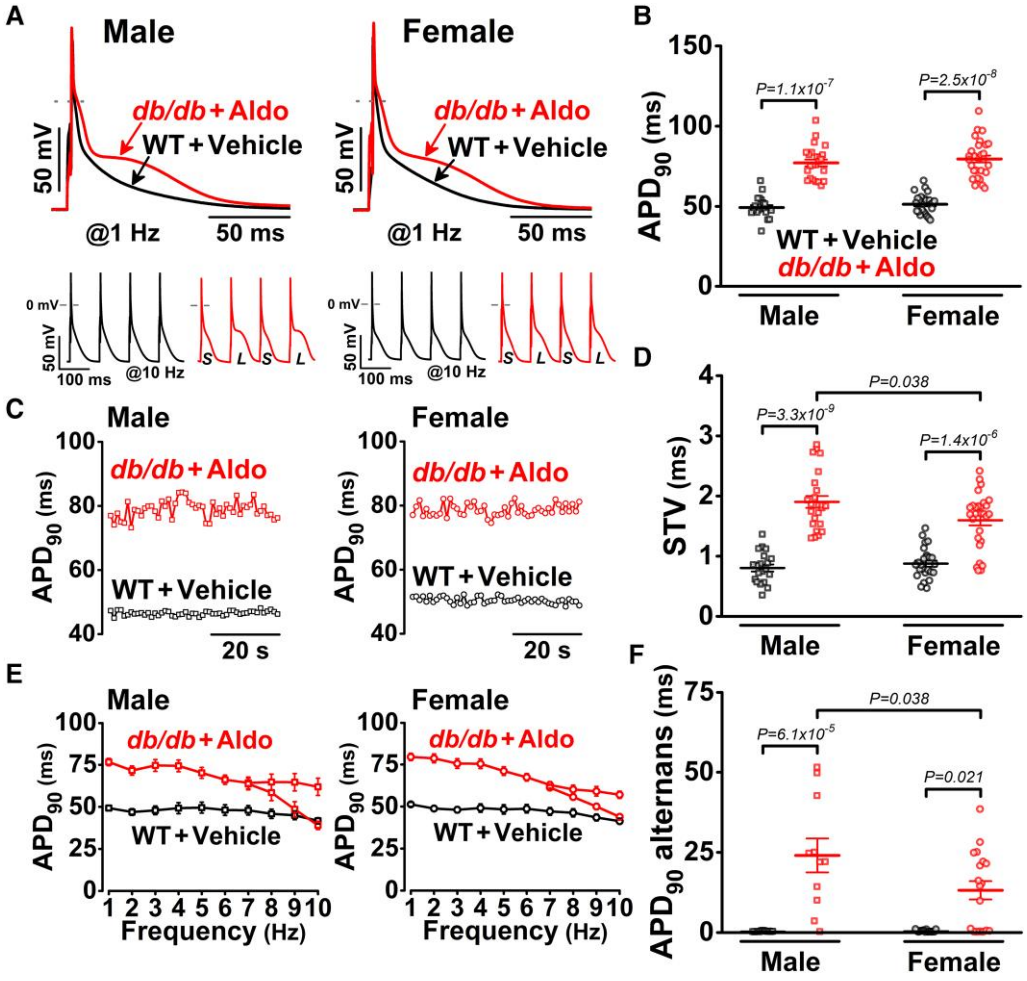

Figure 5 Sex differences in arrhythmogenic APs in HFpEF cardiomyocytes. (*A*) Representative ventricular APs in male and female *db/db* mice with chronic aldosterone infusion (*db/db* + Aldo) vs. vehicle-treated WT control (WT + vehicle) cardiomyocytes paced at 1 Hz (above). Tachypacing (10 Hz) induced APD alternans (S, short; L, long) in *db/db* + Aldo (inset, below). (*B*) APD at 90% repolarization (APD_{90}). (*C*) Fifty consecutive APD_{90} values at 1 Hz pacing. (*D*) Increased STV of APD_{90} in *db/db* + Aldo. *n* (cells)/*N* (animals) = 20/7 for WT + vehicle male, 25/8 for WT + vehicle female, 24/8 for *db/db* + Aldo male, and 29/8 for *db/db* + Aldo female (for both APD_{90} and STV). (*E*) Frequency dependence of APD_{90}. (*F*) Amplitude of APD_{90} alternans at 10 Hz tachypacing. *n* (cells)/*N* (animals) = 13/7 for WT + vehicle male, 16/8 for WT + vehicle female, 11/7 for *db/db* + Aldo male, and 18/8 for *db/db* + Aldo female. Hierarchical (nested) ANOVA followed by Šídák's multiple comparisons test.

humans, we found that female *db/db* + Aldo mice exhibited lower BNP levels (*Figure 1*) and more severe diastolic dysfunction (*Figure 2*). Important to note is that female homozygous *db/db* mice are infertile and exhibit markedly reduced oestrogen levels by 8 weeks of age and extensive ovarian follicular involution by 16 weeks of age.[44] Thus, even though we used young adult (16-week-old) *db/db* + Aldo mice, the hormonal status of these female mice could be a proxy of the post-menopausal stage, which agrees with clinical observations that HFpEF is more predominant and characterized by more severe diastolic dysfunction in post-menopausal women.[3]

Diastolic dysfunction is a core characteristic of HFpEF, although it is also frequently present in HFrEF, and several mechanisms have been implicated specific to cardiomyocytes (e.g. impairments of myofilaments, Ca^{2+} handling, and energetics) and non-cardiomyocytes (e.g. inflammation, fibrosis, and microvascular dysfunction).[45] We found key myofilament alterations in female *db/db* + Aldo ventricles, including increased expression of N2B titin isoform, and increased phosphorylation of titin's PEVK spring element at S170 site, which is a target for both PKC and CaMKII, and both increase titin's stiffness (in contrast to PKA phosphorylation of titin, which reduces titin's stiffness).[32,33,46] Sex differences in inflammation and fibrosis are well established in HFpEF. More fibrosis has been shown in diabetic HFpEF hearts,[47] and greater cardiac remodelling in female patients with diabetes and HFpEF[24] and in female *db/db* mice.[25] In line with this, we found a trend for increased periostin expression in female *db/db* + Aldo hearts. Troponin-I S22/23 phosphorylation was reduced in *db/db* + Aldo female vs. male hearts, which increases myofilament Ca^{2+} sensitivity and could contribute to diastolic dysfunction. Impairments in cardiac mitochondrial function also contribute to differential diastolic dysfunction between sexes.[20] We have also previously reported a marked increase in vascular myogenic tone in *db/db* + Aldo mice that could contribute to hypertension, highlighting a critical vascular derangement in HFpEF.[23] Nonetheless, the exact contribution of other cell types in the heart to diastolic dysfunction requires further investigation.[45]

Diastolic Ca^{2+} handling impairments may also be involved in diastolic dysfunction in HFpEF.[48] Reduced Ca^{2+} removal rate and reduced expression of the sarco/endoplasmic reticulum Ca^{2+} ATPase (SERCA) were observed only in diabetic Zucker fatty and spontaneously hypertensive (ZSF1)

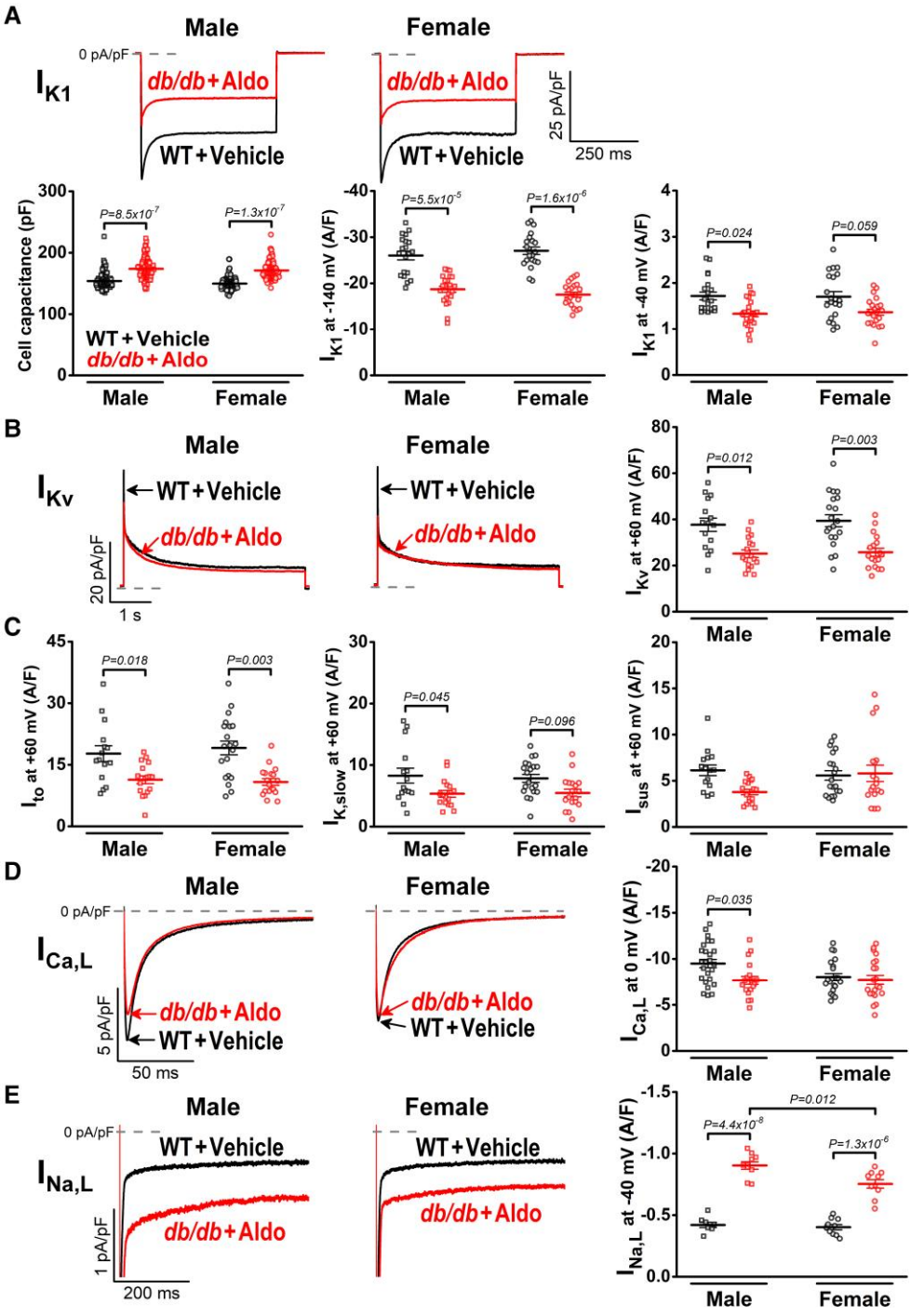

Figure 6 Sex-dependent remodelling in K^+ currents, L-type Ca^{2+} current, and late Na^+ current in HFpEF cardiomyocytes. (*A*) Representative inward rectifier K^+ current (I_{K1}) traces at −140 mV in male and female *db/db* mice with chronic aldosterone infusion (*db/db* + Aldo) vs. vehicle-treated WT control (WT + vehicle) cardiomyocytes. Increased cell capacitance and reduced I_{K1} densities at −140 and −40 mV in *db/db* + Aldo in both sexes. *n* (cells)/*N* (animals) = 97/8 for WT + vehicle male, 112/8 for WT + vehicle female, 110/8 for *db/db* + Aldo male, and 109/8 for *db/db* + Aldo female. (*B*) Representative voltage-gated K^+ current (I_{Kv}) traces. The net I_{Kv} current was reduced in both sexes in HFpEF. (*C*) Transient outward K^+ current (I_{to}), slowly inactivating K^+ current ($I_{K,slow}$), and sustained K^+ current (I_{sus}) were separated by biexponential fitting to I_{Kv} traces. *n* (cells)/*N* (animals) = 15/5 for WT + vehicle male, 20/6 for WT + vehicle female, 17/6 for *db/db* + Aldo male, and 18/6 for *db/db* + Aldo female. (*D*) Representative L-type Ca^{2+} current ($I_{Ca,L}$) traces. $I_{Ca,L}$ was reduced only in male *db/db* + Aldo cardiomyocytes. *n* (cells)/*N* (animals) = 25/7 for WT + vehicle male, 21/8 for WT + vehicle female, 19/8 for *db/db* + Aldo male, and 21/8 for *db/db* + Aldo female. (*E*) Representative late Na^+ current ($I_{Na,L}$) traces. $I_{Na,L}$ was markedly upregulated in *db/db* + Aldo, and the increase was larger in male than in female cardiomyocytes. *n* (cells)/*N* (animals) = 8/4 for WT + vehicle male, 10/5 for WT + vehicle female, 10/6 for *db/db* + Aldo male, and 10/6 for *db/db* + Aldo female. Hierarchical (nested) ANOVA followed by Šídák's multiple comparisons test.

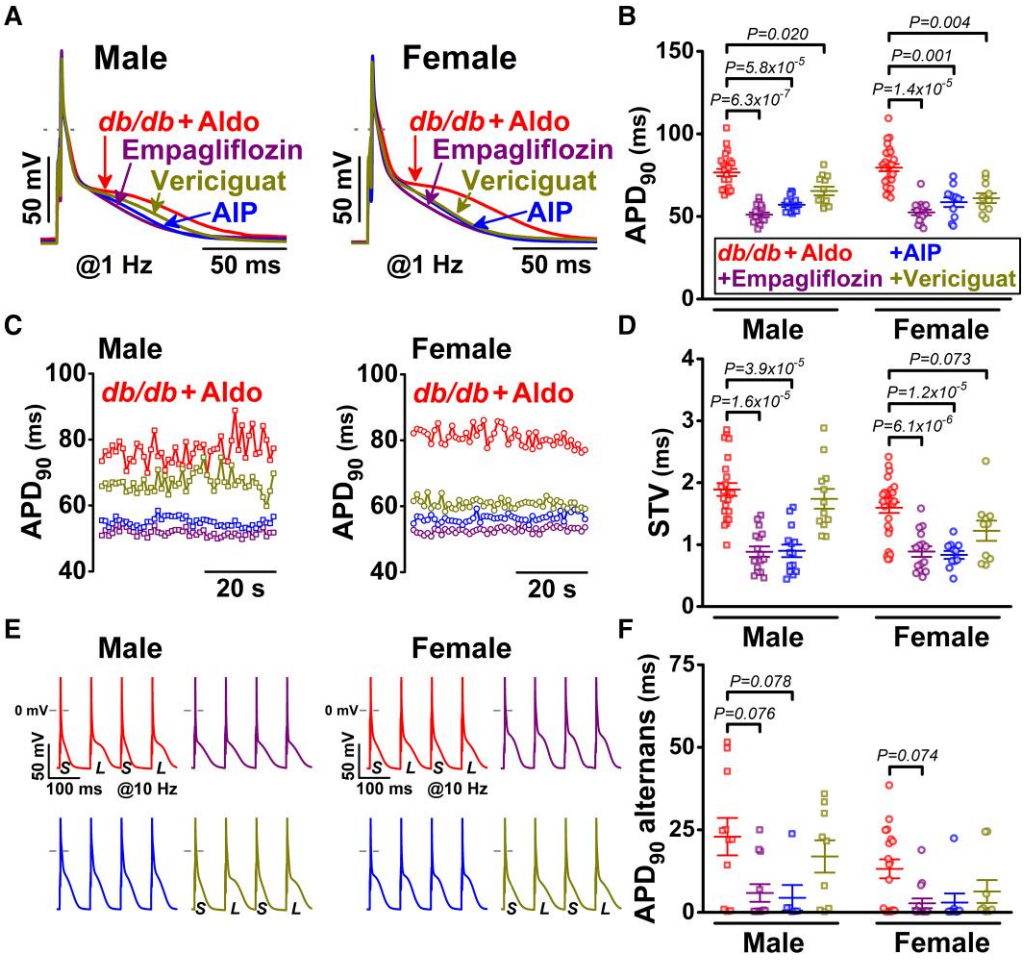

Figure 7 Sex-dependent electrophysiological responses to therapeutic interventions in HFpEF cardiomyocytes. (*A*) Representative ventricular APs at 1 Hz pacing in male and female *db/db* mice with chronic aldosterone infusion (*db/db* + Aldo) in control and following cell pre-treatments with empagliflozin, AIP, and vericiguat. (*B*) Attenuation of prolonged APD at 90% repolarization (APD_{90}) by empagliflozin, AIP, and vericiguat. (*C*) Fifty consecutive APD_{90} values at 1 Hz pacing. (*D*) Increased STV of APD_{90} in *db/db* + Aldo was reversed by empagliflozin and AIP in both sexes. Vericiguat reduced STV only in female *db/db* + Aldo cardiomyocytes. *n* (cells)/*N* (animals) = 24/8 for control male, 29/8 for control female, 16/6 for empagliflozin-treated male, 15/6 for empagliflozin-treated female, 14/4 for AIP-treated male, 11/4 for AIP-treated female, 12/4 for vericiguat-treated male, and 10/4 for vericiguat-treated female. (*E*) Representative APD_{90} alternans during 10 Hz pacing (S, short; L, long). (*F*) APD_{90} alternans was markedly reduced by empagliflozin and AIP in both sexes. Vericiguat reduced APD_{90} alternans only in female *db/db* + Aldo cardiomyocytes. *n* (cells)/*N* (animals) = 11/7 for control male, 18/8 for control female, 12/5 for empagliflozin-treated male, 20/6 for empagliflozin-treated female, 6/4 for AIP-treated male, 8/4 for AIP-treated female, 9/4 for vericiguat-treated male, and 9/4 for vericiguat-treated female. Hierarchical (nested) ANOVA followed by Dunnett's multiple comparisons test.

rats but not in Dahl salt-sensitive (DSS) rats, suggesting that this could be specific to diabetic HFpEF.[49] In line with this, we have previously reported that diastolic [Ca^{2+}] was increased and that CaT decay was prolonged in the diabetic *db/db* + Aldo mice.[23] However, interestingly, we showed here that these CaT changes were only observed in male but not in female *db/db* + Aldo mice (*Figure 3*), while females had worse diastolic dysfunction (*Figure 2*) and myofilament alterations (*Figure 4*). These data suggest that Ca^{2+} handling impairments in male *db/db* + Aldo mice and myofilament and extracellular matrix remodelling in female *db/db* + Aldo mice may importantly mediate the diastolic dysfunction.

Arrhythmias (both atrial and ventricular) frequently occur in patients with HFpEF, although until recently, HFpEF has not been considered an arrhythmogenic disease. Non-sustained ventricular tachycardia is common, present in 30–45% patients with HFpEF, whereas atrial fibrillation occurs in roughly two-thirds of patients with HFpEF.[12,50,51] Ventricular arrhythmias are more common in male patients with HFpEF,[10] and their prevalence is even higher in the presence of diabetes.[11] The heart rate-corrected QT interval (QTc) in HFpEF is generally prolonged[51] and associated with more severe diastolic dysfunction.[52] Male DSS rats exhibited longer QT intervals and increased SCD due to ventricular arrhythmias compared to females.[53] In ventricular cardiomyocytes, APD prolongation has previously been shown both in DSS rats[37] and in HFD + L-NAME–treated mice,[19] similar to our findings here in *db/db* + Aldo mice (*Figure 5*). In addition to QT prolongation, microvolt T-wave alternans was also a significant predictor of arrhythmic events in patients with chronic myocardial infarction and a preserved EF.[54] Here, we reported marked mechanical (see Supplementary material online, *Figure S6*) and electrical (*Figure 5*) alternans in *db/db* + Aldo with greater alternans amplitudes seen in male HFpEF mice. Furthermore, DADs represent important arrhythmia triggers, and DADs were enhanced in *db/db* + Aldo mice (see Supplementary material online, *Figure S7*) in line with previous data in DSS rats.[37]

Prolonged QT and APD indicate an impaired repolarization process of the myocardium. In HFpEF, an enhanced response of QT interval lengthening to the class III antiarrhythmic ibutilide was reported even in patients

with a normal QT interval vs. age- and sex-matched control individuals without HF.[55] This suggests blunted repolarization reserve mechanisms in HFpEF. Downregulation of voltage-gated K^+ currents, including I_{to}, I_{Kr}, and I_{K1} (by ~50, ~60, and ~55%, respectively), has previously been reported in male DSS rats.[37] Here, in *db/db* + Aldo mice, we found ~45–50% reduction in I_{to} and ~30–35% reduction in I_{K1}, both without significant sex difference (*Figure 6*). This extent of I_{to} downregulation in *db/db* + Aldo mice is similar to that reported previously in HFrEF cardiomyocytes, whereas I_{K1} downregulation was more pronounced in HFrEF (~50% reduction in I_{K1}) than in HFpEF.[56] $I_{K,slow}$ was significantly reduced only in male *db/db* + Aldo myocytes. Changes in depolarizing currents can also affect APD and arrhythmias. $I_{Ca,L}$ was upregulated (by ~25%) in parallel with increased CaT amplitude and SR Ca^{2+} load in male DSS rats,[37,57] which may represent a compensatory response to mechanical afterload.[58,59] In contrast to this, $I_{Ca,L}$ was reduced (by ~20%) in male *db/db* + Aldo mice, and $I_{Ca,L}$ was unchanged in females (*Figure 6*). However, $I_{Na,L}$ was markedly upregulated in *db/db* + Aldo mice (*Figure 6*), and larger $I_{Na,L}$ enhancement was found in males (by ~115%) compared to females (by ~85%). Pathological $I_{Na,L}$ upregulation has also been shown in human cardiomyocytes from patients with aortic stenosis and a HFpEF-like phenotype[60] and in the HFD + L-NAME HFpEF mice.[19]

Although we found minor Ca^{2+} handling impairments in *db/db* + Aldo (*Figure 3*), which was significant only in males, CaMKII inhibition had marked effects on APD and DADs in both sexes (*Figure 7*). This suggests that CaMKII is activated in HFpEF, but its activation may be promoted by post-translational modifications (e.g. oxidation and *O*-GlcNAcylation) rather than simply canonical Ca^{2+}/calmodulin binding.[29] CaMKII activation has previously been shown in diabetic hyperglycaemia (via *O*-GlcNAcylation), where its electrophysiological effects were prevented in knock-in mice in which the key CaMKII *O*-GlcNAcylation site was ablated (S280A).[30] CaMKII appears also to mediate adverse cardiac effects of aldosterone (via oxidation).[61] Chronic CaMKII overactivation affects arrhythmogenicity and contributes to cardiac hypertrophic remodelling, fibrosis, and inflammation and modulates the stiffness of the myocardium via phosphorylating titin.[29,32] Thus, CaMKII signalling may play a key role, not only in HFrEF and diabetes but also in HFpEF. Further studies are required to elucidate the exact role and regulation of CaMKII in HFpEF.

Empagliflozin also reversed all arrhythmogenic APD changes in both sexes (*Figure 7*, Supplementary material online, *Figure S8*). In line with these pre-clinical benefits, empagliflozin improved cardiovascular outcomes in HFpEF similarly in men and women.[27] It was previously shown that empagliflozin fully reversed the pathological $I_{Na,L}$ upregulation in both human and murine HFpEF cardiomyocytes.[19,60] This effect of empagliflozin on $I_{Na,L}$ was again similar to the CaMKII inhibitor AIP suggesting that empagliflozin may act via limiting CaMKII signalling.[19,60,62] Empagliflozin reduced CaMKII autophosphorylation and phosphorylation of RyR2 at serine 2814 (a CaMKII target site), and attenuated Ca sparks and waves in *db/db* and TAC mice and failing human cardiomyocytes.[63,64] Interestingly, these empagliflozin effects required longer cell pre-incubations (30 min–4 h), and shorter empagliflozin treatment did not affect CaMKII activity and Ca^{2+} handling in HFrEF myocytes[63] nor inhibit $I_{Na,L}$ in HFpEF myocytes.[19] These data suggest that the target of empagliflozin in cardiomyocytes could be upstream of CaMKII. Empagliflozin's clinical target, SGLT2, is not expressed in cardiomyocytes, but its beneficial effects in isolated myocytes have been attributed to reduction in ROS production, inhibition of Na^+/H^+ exchanger and I_{NaL};[65] however, details remain controversial.[62,66] Nonetheless, Na^+ and Ca^{2+} handling impairments are tightly connected forming a vicious cycle through an $I_{Na,L}$–ROS–CaMKII–leak RyR-mediated feedback in HF,[35] and empagliflozin may target one component of this vicious cycle, which calls for additional mechanistic investigations.

Vericiguat had minimal effects on HFpEF myocyte proarrhythmia, and these effects were only observed in female *db/db* + Aldo cardiomyocytes (*Figure 7*). Lower BNP levels in HFpEF females clinically[67] and in our mouse model (*Figure 1*) could limit NO production and reduce activation of sGC–cGMP–PKG signalling. Thus, vericiguat, a direct sGC stimulator, may be able to further activate PKG in females. The vericiguat-induced shortening of APD in female *db/db* + Aldo myocytes might be explained by a PKG-dependent phosphorylation of the L-type Ca^{2+} channel that reduces $I_{Ca,L}$ amplitude.[68] The ineffectiveness of vericiguat in *db/db* + Aldo males might be due to a 'ceiling' effect, meaning that PKG might already be maximally activated, or alternatively, it is desensitized to cGMP. Nonetheless, vericiguat treatment in patients with HFpEF failed to improve quality of life in both sexes.[28] However, neprilysin inhibition also stimulates sGC–cGMP–PKG signalling via augmentation of the natriuretic peptides, and sacubitril/valsartan, an angiotensin receptor/neprilysin inhibitor, reduced HF hospitalization only in female patients with HFpEF,[69] which would be in line with an impaired BNP–NO–sGC–cGMP–PKG pathway in women.

In conclusion, here, we provided evidence that the *db/db* + Aldo pre-clinical HFpEF murine model has large potential for clinical translation as it recapitulates fundamental sex-specific features in HFpEF, i.e. worse diastolic dysfunction in females but higher arrhythmia susceptibility in males. We also showed key sex differences in myofilament proteins, Ca^{2+} handling, ionic currents, and proarrhythmic AP remodelling in HFpEF. We also tested for sex-specific antiarrhythmic responses to clinically used drugs (empagliflozin, vericiguat) and selective CaMKII inhibition. Future studies are required to further our mechanistic understanding of HFpEF cardiomyocyte signalling mechanisms, which are inherently complex,[16] and here, we only discussed the potential roles of CaMKII and PKG-dependent pathways in HFpEF cardiomyocyte proarrhythmia.

4.1. Limitations

Here, we focused on sex differences in cardiomyocyte excitation–contraction coupling mechanisms and electrophysiology in an obese diabetic HFpEF mouse model. Further investigations are required to identify the exact mechanisms of diastolic dysfunction, including more detailed myofilament studies, and assessing microtubule detyrosination, tissue-level changes (fibrosis and extracellular matrix remodelling), and the role of non-cardiomyocytes in HFpEF, which may reveal additional sex differences in pre-clinical HFpEF animals and human HFpEF. Future *in vivo* arrhythmia tests may inform about exact arrhythmia risk, and *in vivo* chronic drug treatments may reveal potential reverse remodelling that attenuates arrhythmogenicity and diastolic dysfunction in HFpEF.

Translational perspective

Sex differences in susceptibility to diastolic dysfunction and arrhythmias have been observed in HFpEF patients, but mechanisms are incompletely understood. Here, we show that obese diabetic HFpEF mice recapitulate these key sex-dependent differences and exhibit differential ionic and myofilament remodelling between sexes. Our results could (i) improve the mechanistic understanding of cardiomyocyte excitation–contraction coupling contributing to HFpEF between sexes, (ii) indicate key sex-dependent differences in cardiomyocyte proarrhythmic mechanisms, and (iii) suggest a key role for CaMKII inhibition and empagliflozin in attenuating cellular proarrhythmia in HFpEF.

Supplementary material

Supplementary material is available at *Cardiovascular Research* online.

Acknowledgements

We thank Carolyn Sui, Anastasia Krajnovic, and Megan Ngim for their help in animal care, tissue collection, and laboratory tasks.

Conflict of interest: none declared.

Funding

This work was supported by grants from the National Institutes of Health P01-HL141084 (D.M.B.), R01-HL142282 (D.M.B. and J.B.), and R35-HL144998 (H.G.); the American Heart Association 23CDA1051603 (B.H.); the Stanford Diabetes Research Center P30DK116074 (B.H. and D.M.B.); and the **Ministerio de Ciencia, Tecnología e Innovación (MinCiencias-Colombia)** (J.M.H.); and the Fulbright Colombia scholarship (J.M.H.).

Data availability

The data underlying this article will be shared upon reasonable request to the corresponding authors.

References

1. Regitz-Zagrosek V, Kararigas G. Mechanistic pathways of sex differences in cardiovascular disease. *Physiol Rev* 2017;**97**:1–37.
2. Lam CSP, Arnott C, Beale AL, Chandramouli C, Hilfiker-Kleiner D, Kaye DM, Ky B, Santema BT, Sliwa K, Voors AA. Sex differences in heart failure. *Eur Heart J* 2019;**40**:3859–3868c.
3. DeFilippis EM, Beale A, Martyn T, Agarwal A, Elkayam U, Lam CSP, Hsich E. Heart failure subtypes and cardiomyopathies in women. *Circ Res* 2022;**130**:436–454.
4. Jin X, Chandramouli C, Allocco B, Gong E, Lam CSP, Yan LL. Women's participation in cardiovascular clinical trials from 2010 to 2017. *Circulation* 2020;**141**:540–548.
5. Beale AL, Meyer P, Marwick TH, Lam CSP, Kaye DM. Sex differences in cardiovascular pathophysiology: why women are overrepresented in heart failure with preserved ejection fraction. *Circulation* 2018;**138**:198–205.
6. Sotomi Y, Hikoso S, Nakatani D, Mizuno H, Okada K, Dohi T, Kitamura T, Sunaga A, Kida H, Oeun B, Sato T, Komukai S, Tamaki S, Yano M, Hayashi T, Nakagawa A, Nakagawa Y, Yasumura Y, Yamada T, Sakata Y; PURSUIT-HFpEF Investigators. Sex differences in heart failure with preserved ejection fraction. *J Am Heart Assoc* 2021;**10**:e018574.
7. Ciccarelli M, Dawson D, Falcao-Pires I, Giacca M, Hamdani N, Heymans S, Hooghiemstra A, Leeuwis A, Hermkens D, Tocchetti CG, van der Velden J, Zacchigna S, Thum T. Reciprocal organ interactions during heart failure: a position paper from the ESC Working Group on Myocardial Function. *Cardiovasc Res* 2021;**117**:2416–2433.
8. Levy D, Larson MG, Vasan RS, Kannel WB, Ho KK. The progression from hypertension to congestive heart failure. *JAMA* 1996;**275**:1557–1562.
9. Kannel WB, Hjortland M, Castelli WP. Role of diabetes in congestive heart failure: the Framingham study. *Am J Cardiol* 1974;**34**:29–34.
10. Curtain JP, Adamson C, Kondo T, Butt JH, Desai AS, Zannad F, Rouleau JL, Rohde LE, Kober L, Anand IS, van Veldhuisen DJ, Zile MR, Lefkowitz MP, Solomon SD, Packer M, Petrie MC, Jhund PS, McMurray JJV. Investigator-reported ventricular arrhythmias and mortality in heart failure with mildly reduced or preserved ejection fraction. *Eur Heart J* 2023;**44**:668–677.
11. Vaduganathan M, Claggett BL, Chatterjee NA, Anand IS, Sweitzer NK, Fang JC, O'Meara E, Shah SJ, Hegde SM, Desai AS, Lewis EF, Rouleau J, Pitt B, Pfeffer MA, Solomon SD. Sudden death in heart failure with preserved ejection fraction: a competing risks analysis from the TOPCAT Trial. *JACC Heart Fail* 2018;**6**:653–661.
12. Shah SJ, Borlaug BA, Kitzman DW, McCulloch AD, Blaxall BC, Agarwal R, Chirinos JA, Collins S, Deo RC, Gladwin MT. Research priorities for heart failure with preserved ejection fraction: National Heart, Lung, and Blood Institute Working Group summary. *Circulation* 2020;**141**:1001–1026.
13. Blenck CL, Harvey PA, Reckelhoff JF, Leinwand LA. The importance of biological sex and estrogen in rodent models of cardiovascular health and disease. *Circ Res* 2016;**118**:1294–1312.
14. Ramirez FD, Motazedian P, Jung RG, Di Santo P, MacDonald Z, Simard T, Clancy AA, Russo JJ, Welch V, Wells GA, Hibbert B. Sex bias is increasingly prevalent in preclinical cardiovascular research: implications for translational medicine and health equity for women: a systematic assessment of leading cardiovascular journals over a 10-year period. *Circulation* 2017;**135**:625–626.
15. Valero-Munoz M, Backman W, Sam F. Murine models of heart failure with preserved ejection fraction: a "fishing expedition". *JACC Basic Transl Sci* 2017;**2**:770–789.
16. Mishra S, Kass DA. Cellular and molecular pathobiology of heart failure with preserved ejection fraction. *Nat Rev Cardiol* 2021;**18**:400–423.
17. Withaar C, Lam CSP, Schiattarella GG, de Boer RA, Meems LMG. Heart failure with preserved ejection fraction in humans and mice: embracing clinical complexity in mouse models. *Eur Heart J* 2021;**42**:4420–4430.
18. Schiattarella GG, Altamirano F, Tong D, French KM, Villalobos E, Kim SY, Luo X, Jiang N, May HI, Wang ZV, Hill TM, Mammen PPA, Huang J, Lee DI, Hahn VS, Sharma K, Kass DA, Lavandero S, Gillette TG, Hill JA. Nitrosative stress drives heart failure with preserved ejection fraction. *Nature* 2019;**568**:351–356.
19. Hegyi B, Mira Hernandez J, Shen EY, Habibi NR, Bossuyt J, Bers DM. Empagliflozin reverses late Na^+ current enhancement and cardiomyocyte proarrhythmia in a translational murine model of heart failure with preserved ejection fraction. *Circulation* 2022;**145**:1029–1031.
20. Cao Y, Vergnes L, Wang YC, Pan C, Chella Krishnan K, Moore TM, Rosa-Garrido M, Kimball TH, Zhou Z, Charugundla S, Rau CD, Seldin MM, Wang J, Wang Y, Vondriska TM, Reue K, Lusis AJ. Sex differences in heart mitochondria regulate diastolic dysfunction. *Nat Commun* 2022;**13**:3850.
21. Tong D, Schiattarella GG, Jiang N, May HI, Lavandero S, Gillette TG, Hill JA. Female sex is protective in a preclinical model of heart failure with preserved ejection fraction. *Circulation* 2019;**140**:1769–1771.
22. Roh J, Hill JA, Singh A, Valero-Munoz M, Sam F. Heart failure with preserved ejection fraction: heterogeneous syndrome, diverse preclinical models. *Circ Res* 2022;**130**:1906–1925.
23. Hegyi B, Mira Hernandez J, Ko CY, Hong J, Shen EY, Spencer ER, Smoliarchuk D, Navedo MF, Bers DM, Bossuyt J. Diabetes and excess aldosterone promote heart failure with preserved ejection fraction. *J Am Heart Assoc* 2022;**11**:e027164.
24. Shi K, Yang MX, Huang S, Yan WF, Qian WL, Li Y, Guo YK, Yang ZG. Effect of diabetes mellitus on the development of left ventricular contractile dysfunction in women with heart failure and preserved ejection fraction. *Cardiovasc Diabetol* 2021;**20**:185.
25. Alex L, Russo I, Holoborodko V, Frangogiannis NG. Characterization of a mouse model of obesity-related fibrotic cardiomyopathy that recapitulates features of human heart failure with preserved ejection fraction. *Am J Physiol Heart Circ Physiol* 2018;**315**:H934–H949.
26. Merrill M, Sweitzer NK, Lindenfeld J, Kao DP. Sex differences in outcomes and responses to spironolactone in heart failure with preserved ejection fraction: a secondary analysis of TOPCAT Trial. *JACC Heart Fail* 2019;**7**:228–238.
27. Butler J, Filippatos G, Siddiqi TJ, Ferreira JP, Brueckmann M, Bocchi E, Bohm M, Chopra VK, Giannetti N, Iwata T, Januzzi JL, Kaul S, Pina IL, Ponikowski P, Rauch-Krohnert U, Shah SJ, Senni M, Sumin M, Verma S, Zhang J, Pocock SJ, Zannad F, Packer M, Anker SD. Effects of empagliflozin in women and men with heart failure and preserved ejection fraction. *Circulation* 2022;**146**:1046–1055.
28. Armstrong PW, Lam CSP, Anstrom KJ, Ezekowitz J, Hernandez AF, O'Connor CM, Pieske B, Ponikowski P, Shah SJ, Solomon SD, Voors AA, She L, Vlajnic V, Carvalho F, Bamber L, Blaustein RO, Roessig L, Butler J; VITALITY-HFpEF Study Group. Effect of vericiguat vs placebo on quality of life in patients with heart failure and preserved ejection fraction: the VITALITY-HFpEF randomized clinical trial. *JAMA* 2020;**324**:1512–1521.
29. Hegyi B, Bers DM, Bossuyt J. CaMKII signaling in heart diseases: emerging role in diabetic cardiomyopathy. *J Mol Cell Cardiol* 2019;**127**:246–259.
30. Hegyi B, Fasoli A, Ko CY, Van BW, Alim CC, Shen EY, Ciccozzi MM, Tapa S, Ripplinger CM, Erickson JR, Bossuyt J, Bers DM. CaMKII serine 280 O-GlcNAcylation links diabetic hyperglycemia to proarrhythmia. *Circ Res* 2021;**129**:98–113.
31. Bers DM. Cardiac excitation-contraction coupling. *Nature* 2002;**415**:198–205.
32. Hidalgo C, Hudson B, Bogomolovas J, Zhu Y, Anderson B, Greaser M, Labeit S, Granzier H. PKC phosphorylation of titin's PEVK element: a novel and conserved pathway for modulating myocardial stiffness. *Circ Res* 2009;**105**:631–638, 17 p following 638.
33. Hidalgo CG, Chung CS, Saripalli C, Methawasin M, Hutchinson KR, Tsaprailis G, Labeit S, Mattiazzi A, Granzier HL. The multifunctional Ca(2+)/calmodulin-dependent protein kinase II delta (CaMKIIdelta) phosphorylates cardiac titin's spring elements. *J Mol Cell Cardiol* 2013;**54**:90–97.
34. Oka T, Xu J, Kaiser RA, Melendez J, Hambleton M, Sargent MA, Lorts A, Brunskill EW, Dorn GW II, Conway SJ, Aronow BJ, Robbins J, Molkentin JD. Genetic manipulation of periostin expression reveals a role in cardiac hypertrophy and ventricular remodeling. *Circ Res* 2007;**101**:313–321.
35. Hegyi B, Polonen RP, Hellgren KT, Ko CY, Ginsburg KS, Bossuyt J, Mercola M, Bers DM. Cardiomyocyte Na^+ and Ca^{2+} mishandling drives vicious cycle involving CaMKII, ROS, and ryanodine receptors. *Basic Res Cardiol* 2021;**116**:58.
36. Qu Z, Weiss JN. Cardiac alternans: from bedside to bench and back. *Circ Res* 2023;**132**:127–149.
37. Cho JH, Zhang R, Kilfoil PJ, Gallet R, de Couto G, Bresee C, Goldhaber JI, Marban E, Cingolani E. Delayed repolarization underlies ventricular arrhythmias in rats with heart failure and preserved ejection fraction. *Circulation* 2017;**136**:2037–2050.
38. Hegyi B, Morotti S, Liu C, Ginsburg KS, Bossuyt J, Belardinelli L, Izu LT, Chen-Izu Y, Banyasz T, Grandi E, Bers DM. Enhanced depolarization drive in failing rabbit ventricular myocytes: calcium-dependent and beta-adrenergic effects on late sodium, L-type calcium, and sodium-calcium exchange currents. *Circ Arrhythm Electrophysiol* 2019;**12**:e007061.
39. Johnson DM, Heijman J, Bode EF, Greensmith DJ, van der Linde H, Abi-Gerges N, Eisner DA, Trafford AW, Volders PG. Diastolic spontaneous calcium release from the sarcoplasmic reticulum increases beat-to-beat variability of repolarization in canine ventricular myocytes after beta-adrenergic stimulation. *Circ Res* 2013;**112**:246–256.
40. McHugh K, DeVore AD, Wu J, Matsouaka RA, Fonarow GC, Heidenreich PA, Yancy CW, Green JB, Altman N, Hernandez AF. Heart failure with preserved ejection fraction and diabetes: JACC state-of-the-art review. *J Am Coll Cardiol* 2019;**73**:602–611.

41. Edelmann F, Tomaschitz A, Wachter R, Gelbrich G, Knoke M, Dungen HD, Pilz S, Binder L, Stahrenberg R, Schmidt A, Marz W, Pieske B. Serum aldosterone and its relationship to left ventricular structure and geometry in patients with preserved left ventricular ejection fraction. *Eur Heart J* 2012;**33**:203–212.
42. Wang B, Chandrasekera PC, Pippin JJ. Leptin- and leptin receptor-deficient rodent models: relevance for human type 2 diabetes. *Curr Diabetes Rev* 2014;**10**:131–145.
43. Packer M. Leptin-aldosterone-neprilysin axis: identification of its distinctive role in the pathogenesis of the three phenotypes of heart failure in people with obesity. *Circulation* 2018;**137**:1614–1631.
44. Garris DR, Garris BL. Diabetes (db/db) mutation-induced ovarian involution: progressive hypercytolipidemia. *Exp Biol Med (Maywood)* 2003;**228**:1040–1050.
45. Grandi E, Navedo MF, Saucerman JJ, Bers DM, Chiamvimonvat N, Dixon RE, Dobrev D, Gomez AM, Harraz OF, Hegyi B, Jones DK, Krogh-Madsen T, Murfee WL, Nystoriak MA, Posnack NG, Ripplinger CM, Veeraraghavan R, Weinberg S. Diversity of cells and signals in the cardiovascular system. *J Physiol* 2023;**601**:2547–2592.
46. Hamdani N, Herwig M, Linke WA. Tampering with springs: phosphorylation of titin affecting the mechanical function of cardiomyocytes. *Biophys Rev* 2017;**9**:225–237.
47. Lejeune S, Roy C, Slimani A, Pasquet A, Vancraeynest D, Vanoverschelde JL, Gerber BL, Beauloye C, Pouleur AC. Diabetic phenotype and prognosis of patients with heart failure and preserved ejection fraction in a real life cohort. *Cardiovasc Diabetol* 2021;**20**:48.
48. Johnson DM, Pavlovic D. What is actually preserved in HFpEF? Focus on myocyte calcium handling remodelling. *J Mol Cell Cardiol* 2022;**170**:115–116.
49. Frisk M, Le C, Shen X, Roe AT, Hou Y, Manfra O, Silva GJJ, van Hout I, Norden ES, Aronsen JM, Laasmaa M, Espe EKS, Zouein FA, Lambert RR, Dahl CP, Sjaastad I, Lunde IG, Coffey S, Cataliotti A, Gullestad L, Tonnessen T, Jones PP, Altara R, Louch WE. Etiology-dependent impairment of diastolic cardiomyocyte calcium homeostasis in heart failure with preserved ejection fraction. *J Am Coll Cardiol* 2021;**77**:405–419.
50. Gutierrez A, Ash J, Akdemir B, Alexy T, Cogswell R, Chen J, Adabag S. Nonsustained ventricular tachycardia in heart failure with preserved ejection fraction. *Pacing Clin Electrophysiol* 2020;**43**:1126–1131.
51. Cho JH, Leong D, Cuk N, Ebinger JE, Bresee C, Yoon SH, Ehdaie A, Shehata M, Wang X, Chugh SS, Marban E, Cingolani E. Delayed repolarization and ventricular tachycardia in patients with heart failure and preserved ejection fraction. *PloS One* 2021;**16**:e0254641.
52. Wilcox JE, Rosenberg J, Vallakati A, Gheorghiade M, Shah SJ. Usefulness of electrocardiographic QT interval to predict left ventricular diastolic dysfunction. *Am J Cardiol* 2011;**108**:1760–1766.
53. Elkholey K, Morris L, Niewiadomska M, Houser J, Ramirez M, Tang M, Humphrey MB, Stavrakis S. Sex differences in the incidence and mode of death in rats with heart failure with preserved ejection fraction. *Exp Physiol* 2021;**106**:673–682.
54. Ikeda T, Yoshino H, Sugi K, Tanno K, Shimizu H, Watanabe J, Kasamaki Y, Yoshida A, Kato T. Predictive value of microvolt T-wave alternans for sudden cardiac death in patients with preserved cardiac function after acute myocardial infarction: results of a collaborative cohort study. *J Am Coll Cardiol* 2006;**48**:2268–2274.
55. Tisdale JE, Jaynes HA, Overholser BR, Sowinski KM, Fisch MD, Rodgers JE, Aldemerdash A, Hsu CC, Wang N, Muensterman ET, Rao VU, Kovacs RJ. Enhanced response to drug-induced QT interval lengthening in patients with heart failure with preserved ejection fraction. *J Card Fail* 2020;**26**:781–785.
56. Bossuyt J, Borst JM, Verberckmoes M, Bailey LRJ, Bers DM, Hegyi B. Protein kinase D1 regulates cardiac hypertrophy, potassium channel remodeling, and arrhythmias in heart failure. *J Am Heart Assoc* 2022;**11**:e027573.
57. Kilfoil PJ, Lotteau S, Zhang R, Yue X, Aynaszyan S, Solymani RE, Cingolani E, Marban E, Goldhaber JI. Distinct features of calcium handling and beta-adrenergic sensitivity in heart failure with preserved versus reduced ejection fraction. *J Physiol* 2020;**598**:5091–5108.
58. Shimkunas R, Hegyi B, Jian Z, Shaw JA, Kazemi-Lari MA, Mitra D, Leach JK, Li X, Jaradeh M, Balardi N, Chen YJ, Escobar AL, Baker AJ, Bossuyt J, Banyasz T, Chiamvimonvat N, Lam KS, Bers DM, Izu LT, Chen-Izu Y. Mechanical load regulates excitation-Ca^{2+} signaling-contraction in cardiomyocyte. *Circ Res* 2021;**128**:772–774.
59. Hegyi B, Shimkunas R, Jian Z, Izu LT, Bers DM, Chen-Izu Y. Mechanoelectric coupling and arrhythmogenesis in cardiomyocytes contracting under mechanical afterload in a 3D viscoelastic hydrogel. *Proc Natl Acad Sci U S A* 2021;**118**:e2108484118.
60. Mustroph J, Baier MJ, Pabel S, Stehle T, Trum M, Provaznik Z, Mohler PJ, Musa H, Hund TJ, Sossalla S, Maier LS, Wagner S. Empagliflozin inhibits cardiac late sodium current by Ca/calmodulin-dependent kinase II. *Circulation* 2022;**146**:1259–1261.
61. He BJ, Joiner ML, Singh MV, Luczak ED, Swaminathan PD, Koval OM, Kutschke W, Allamargot C, Yang J, Guan X, Zimmerman K, Grumbach IM, Weiss RM, Spitz DR, Sigmund CD, Blankesteijn WM, Heymans S, Mohler PJ, Anderson ME. Oxidation of CaMKII determines the cardiotoxic effects of aldosterone. *Nat Med* 2011;**17**:1610–1618.
62. Hegyi B, Bers DM. New cardiac targets for empagliflozin: O-GlcNAcylation, CaMKII, and calcium handling. *Am J Physiol Heart Circ Physiol* 2023;**324**:H338–H340.
63. Mustroph J, Wagemann O, Lucht CM, Trum M, Hammer KP, Sag CM, Lebek S, Tarnowski D, Reinders J, Perbellini F, Terracciano C, Schmid C, Schopka S, Hilker M, Zausig Y, Pabel S, Sossalla ST, Schweda F, Maier LS, Wagner S. Empagliflozin reduces Ca/calmodulin-dependent kinase II activity in isolated ventricular cardiomyocytes. *ESC Heart Fail* 2018;**5**:642–648.
64. Kadosaka T, Watanabe M, Natsui H, Koizumi T, Nakao M, Koya T, Hagiwara H, Kamada R, Temma T, Karube F, Fujiyama F, Anzai T. Empagliflozin attenuates arrhythmogenesis in diabetic cardiomyopathy by normalizing intracellular Ca^{2+} handling in ventricular cardiomyocytes. *Am J Physiol Heart Circ Physiol* 2023;**324**:H341–H354.
65. Dyck JRB, Sossalla S, Hamdani N, Coronel R, Weber NC, Light PE, Zuurbier CJ. Cardiac mechanisms of the beneficial effects of SGLT2 inhibitors in heart failure: evidence for potential off-target effects. *J Mol Cell Cardiol* 2022;**167**:17–31.
66. Chung YJ, Park KC, Tokar S, Eykyn TR, Fuller W, Pavlovic D, Swietach P, Shattock MJ. Off-target effects of sodium-glucose co-transporter 2 blockers: empagliflozin does not inhibit Na+/H+ exchanger-1 or lower [Na+]i in the heart. *Cardiovasc Res* 2021;**117**:2794–2806.
67. Harada E, Mizuno Y, Kugimiya F, Shono M, Maeda H, Yano N, Yasue H. Sex differences in heart failure with preserved ejection fraction reflected by B-type natriuretic peptide level. *Am J Med Sci* 2018;**356**:335–343.
68. Yang L, Liu G, Zakharov SI, Bellinger AM, Mongillo M, Marx SO. Protein kinase G phosphorylates Cav1.2 alpha1c and beta2 subunits. *Circ Res* 2007;**101**:465–474.
69. McMurray JJV, Jackson AM, Lam CSP, Redfield MM, Anand IS, Ge J, Lefkowitz MP, Maggioni AP, Martinez F, Packer M, Pfeffer MA, Pieske B, Rizkala AR, Sabarwal SV, Shah AM, Shah SJ, Shi VC, van Veldhuisen DJ, Zannad F, Zile MR, Cikes M, Goncalvesova E, Katova T, Kosztin A, Lelonek M, Sweitzer N, Vardeny O, Claggett B, Jhund PS, Solomon SD. Effects of sacubitril-valsartan versus valsartan in women compared with men with heart failure and preserved ejection fraction: insights from PARAGON-HF. *Circulation* 2020;**141**:338–351.